t = local temperature
T = dimensionless temperature, $t_w - t/t_w - t_c$
u = local axial velocity
U = dimensionless velocity, u/U_c
U_{avg} = average fluid velocity in axial direction
U_c = fluid velocity at pipe center in axial direction
U_{max} = maximum local velocity in axial direction
α = disturbance wave number
β = coefficient of volumetric expansion
μ = liquid viscosity
ρ = liquid density
c = quantity evaluated at $R = 0$
w = quantity evaluated at $R = 1$

LITERATURE CITED

1. Batchelor, G. K., and A. E. Gill, *J. Fluid Mech.*, 14, 529 (1962).
2. Brown, C. K., and W. H. Gauvin, *Can. J. Chem. Eng.*, 43, 306, 313 (1965).
3. Brown, W. G., *VDI Forschungsheft, No. 480* (1960).
4. DeYoung, S. H., and G. F. Scheele, *AIChE J.*, 16, No. 5, 712 (1970).
5. Greene, H. L., *Chem. Eng.*, 73, 22 (1966).
6. Hallman, T. M., *Trans. Am. Soc. Mech. Engrs.*, **78**, 1831 (1956).
7. ———, *N.A.S.A. Tech. Note D-1104* (1961).
8. Hanratty, T. J., E. M. Rosen, and R. L. Kabel, *Ind. Eng. Chem.*, **50**, 815 (1958).
9. Lawrence, W. T., and J. C. Chato, *Trans. Am. Soc. Mech. Engrs. J. Heat Transfer*, **88**, 214 (1966).
10. Metais, B., and E. R. G. Eckert, *ibid.*, **86**, 295 (1964).
11. Morton, B. R., *J. Fluid Mech.*, **8**, 227 (1960).
12. Ostroumov, G. A., *N.A.C.A. Tech. Translation TM 1407* (1958).
13. Pai, S. I., *Report R62SD75*, Space Sciences Laboratory, General Electric (1962).
14. Schade, H., *ASTIA Rept. AD 608096.*
15. Scheele, G. F., and H. L. Greene, *AIChE J.*, **12**, 737 (1966).
16. Scheele, G. F., and T. J. Hanratty, *J. Fluid Mech.*, **14**, 244 (1962).
17. Scheele, G. F., E. M. Rosen, and T. J. Hanratty, *Can. J. Chem. Eng.*, **38**, 67 (1960).
18. Scheele, G. F., unpublished results.
19. Williams, D. B., M.S. thesis, Cornell Univ., Ithaca, N. Y. (1969).

Manuscript received February 1, 1968; revision received April 3, 1969; paper accepted April 7, 1969.

Compressibilities and Virial Coefficients for Methane, Ethylene, and Their Mixtures

ROY C. LEE and WAYNE C. EDMISTER
Oklahoma State University, Stillwater, Oklahoma

A Burnett type of apparatus was built for 12,000 lb./sq.in. pressure and temperatures of 25° to 100°C. Isothermal expansions were run on methane, ethylene, and four binary mixtures at 25°, 50°, and 75°C., and compressibility factors were derived from the pressure ratio observations.

From the experimental data, second and third virial coefficients were derived by two techniques, that is, the slope-intercept and the multiple regressions curve-fit of the data by the density-series virial equation. A comparison of these virial coefficients with those from the different empirical equations of state indicates areas of needed improvements in these equations. Second virial cross coefficients were also obtained.

Compressibility measurements are of great value in providing needed volumetric data for process design calculations and the derivation of thermodynamic properties, such as enthalpy, entropy, and fugacity. In addition to tabulations, analytical formulations (that is, equations of state) are used in presenting real fluid compressibility factors. The purpose of this work is to contribute useful data and correlations of these kinds.

The binary system of methane and ethylene was selected for this study. The compressibility factors for methane, ranging from −274° to 650°F. and from atmospheric pressure to 1,000 atm., have been reported by many investigators (*6, 9, 12, 13, 17, 19, 23* to *26, 28, 32*). Most of the data are for temperatures above ambient. The volumetric properties of ethylene have not been studied as extensively as methane, covering temperatures from −140° to 500°F. and pressures to 3,000 atm., with most of the data above ambient temperatures (*5, 18, 19, 21, 22, 27,*

R. C. Lee is presently at Phillips Petroleum Company, Bartlesville, Oklahoma.

33, 35). Recently, McMath and Edmister (*20*) reported vapor-phase compressibility data for the methane-ethylene system for temperatures from 20° to 60°F. and pressures from 260 to 2,220 lb./sq.in.abs. No other methane-ethylene compressibility data have been published.

ISOTHERMAL EXPANSION METHOD OF BURNETT

The determination of volumetric properties of gases involve making pressure, temperature, volume, and mass measurements. Accurate pressure and temperature measurements are relatively easy to make compared with the others. In 1936, Burnett (*3*) described an isothermal expansion method that required only pressure and temperature measurements to determine the compressibility factors of gases. A high pressure vessel V_1 is filled to a pressure P_0. The gas is expanded into an evacuated vessel V_2, and the pressure P_1 is measured. The gas in V_2 is vented; V_2 is evacuated, and another expansion from V_1 into V_2 is made. The expansions are repeated as many times as desired. The compressibility factor Z_{j-1} before the j^{th} expansion is related to the compressibility factor Z_j after the j^{th} expansion by the following relationship:

$$\frac{P_{j-1}}{P_j} = N\left(\frac{Z_{j-1}}{Z_j}\right) \tag{1}$$

where

$$N = \left(\frac{V_1 + V_2}{V_1}\right)$$

The equations that describe Burnett's expansion method have been presented in detail previously (*24, 31*). The compressibility factor after the j^{th} expansion can be expressed in terms of the volume ratio N, pressure P_j, the compressibility factor Z_0 before the first expansion, and the pressure P_0 before the first expansion:

$$Z_j = N^j\, P_j \left(\frac{Z_0}{P_0}\right) \tag{2}$$

The (volume-ratio) apparatus constant N and the compressibility factor over pressure Z_0/P_0 before the first expansion are found as follows:

$$\underset{P_j \to 0}{\text{Limit}} \left(\frac{P_{j-1}}{P_j}\right) = N \tag{3}$$

and

$$\underset{P_j \to 0}{\text{Limit}}\ N^j P_j = \left(\frac{P_0}{Z_0}\right) \tag{4}$$

Values of Z_j are found from the values of N and P_0/Z_0, thus obtained, by using Equation (2). The above equations apply rigorously only to vessels whose volumes do not change with pressure.

By applying these relationships to the pressure measurements, compressibilities can be determined without making mass or volume measurements. This feature of the method allows it to be used over a wide range of temperatures and pressures. Mueller, Leland, and Kobayaski (*24*) reported compressibility data for methane-hydrogen in the temperature range of −200° to 50°F. and for pressures to 7,000 lb./sq.in.abs. Later, Canfield, Leland, and Kobayashi (*4*) described an apparatus used to obtain data for helium-nitrogen mixtures from 0° to −140°C. Several investigators have described apparatus that have been used for relatively high temperatures. Schneider and several of his associates have reported data to 600°C. (*15, 16, 29, 30*). Witonsky and Miller (*34*) published data for helium-nitrogen mixtures in the temperature range of 175° to 475°C. Thus, the isothermal expansion method of Burnett was chosen as the method to be used to study the volumetric properties for the methane-ethylene system.

DESCRIPTION OF EQUIPMENT

The apparatus consisted of two high pressure bombs, an air thermostat, temperature control and measuring equipment, and pressure measuring equipment.

Air Thermostat

The air thermostat (Figure 1) consisted of a stainless steel dewar containing a squirrel cage blower, cooling coil, electric heaters, rack for holding two bombs and differential-pressure-indicating (DPI) cell, and baffles for directing air flow. The baffles were used to direct the flow of air from the squirrel cage blower, powered by a synchronous motor located outside the thermostat. The air discharged from the blower located above the top baffle passed down a 2-in. tube to the bottom of the dewar. The air passed over a cooling coil through the bottom baffle with four 250-w. strip heaters attached, across the two bombs and DPI cell, and through the top baffle to the blower intake. The baffles, rack, and lid for the dewar were made as a unit and were suspended so that the dewar could be raised to surround them. The dewar was covered with fiber glass insulation.

Temperature Control and Measurement

The temperature of the air thermostat was controlled by subcooling below the desired temperature and by supplying heat with controlled heaters. Two of the 250-w. heaters served as control heaters; the other two were used as auxiliary heaters. For the 25°C. isotherms, the subcooling was achieved by circulating cold water through the cooling coil. For the 50° and 75°C. isotherms, heat losses to the surroundings served as the heat sink.

TABLE 1. COMPOSITION OF GAS SAMPLES

	Nominal composition					
Component	100 CH_4	80 CH_4	60 CH_4	40 CH_4	20 CH_4	100 C_2H_4
			Mole %			
CH_4	99.0	78.8	57.2	38.4	18.4	—
C_2H_4	—	20.7	42.4	61.4	81.6	99.9+
C_2H_6	0.1	0.1	0.1	—	—	—
C_3H_8	0.1	0.4	0.3	0.2	—	—
N_2	0.6					
CO_2	0.2					

TABLE 2. CELL CONSTANTS, N

	Temp., °C.		
Gas system	25	50	75
Methane	1.9432	1.9362	1.9352
80-20	1.9418	1.9356	1.9332
60-40	1.9418	1.9389	1.9371
40-60	1.9424	1.9412	1.9386
20-80	1.9457	1.9443	1.9409
Ethylene	1.9496	1.9505	1.9425

TABLE 3. EXPERIMENTAL COMPRESSIBILITY FACTORS AND COMPARISONS WITH EMPIRICAL EQUATIONS OF STATE: ABRIDGED

		Differences		
Pressure, lb./sq.in.abs.	Z_{Expt}	$\Delta Z_{\mathrm{R\text{-}K}}$	$\Delta Z_{\mathrm{B\text{-}W\text{-}R}}$	$\Delta Z_{\mathrm{G\text{-}B\text{-}W\text{-}R}}$
78.8% methane at 25°C.				
11,598.295	1.6803	−0.11	−0.13	−0.12
2,763.771	0.7541	+0.0020	−0.20	−0.20
1,489.199	0.7890	−0.012	−0.071	−0.073
846.072	0.8704	−0.011	−0.024	−0.025
464.507	0.9279	−0.0074	−0.0091	−0.0099
247.867	0.9615	−0.0043	−0.0039	−0.0043
Std. dev. (18 pt.)		0.031	0.127	0.123
78.8% methane at 50°C.				
11,792.833	1.6192	−0.12	−0.17	−0.17
3,137.596	0.8339	−0.0060	−0.15	−0.16
1,639.056	0.8432	−0.014	−0.054	−0.058
906.546	0.9027	−0.012	−0.020	−0.023
490.696	0.9457	−0.0082	−0.0089	−0.010
260.143	0.9705	−0.0044	−0.0037	−0.0044
Std. dev. (18 pt.)		0.035	0.105	0.108
78.8% methane at 75°C.				
11,991.894	1.6010	−0.13	−0.17	−0.18
3,477.037	0.8974	−0.013	−0.12	−0.12
1,774.702	0.8855	−0.016	−0.043	−0.049
961.334	0.9274	−0.013	−0.018	−0.021
514.382	0.9592	−0.0086	−0.0086	−0.010
271.149	0.9775	−0.0044	−0.0037	−0.0045
Std. dev. (18 pt.)		0.037	0.089	0.095
57.2% methane at 25°C.				
11,963.053	1.7214	−0.13	−0.18	−0.19
2,360.099	0.6594	−0.0047	−0.31	−0.30
1,335.785	0.7248	−0.018	−0.11	−0.11
790.976	0.8334	−0.015	−0.036	−0.035
443.622	0.9076	−0.0092	−0.013	−0.013
238.835	0.9488	−0.0034	−0.0035	−0.0034
Std. dev. (18 pt)		0.037	0.179	−0.176
57.2% methane at 50°C.				
11,829.056	1.6388	−0.086	−0.14	−0.16
2,774.326	0.7452	−0.0003	−0.23	−0.22
1,504.353	0.7835	−0.014	−0.078	−0.079
858.775	0.8672	−0.012	−0.026	−0.027
472.775	0.9261	−0.0079	−0.0097	−0.010
252.944	0.9602	−0.004	−0.0038	−0.0041
Std. dev. (18 pt.)		0.025	0.137	0.138
57.2% methane at 75°C.				
11,931.076	1.6044	−0.090	−0.15	−0.17
3,144.515	0.8191	−0.0046	−0.17	−0.17
1,650.334	0.8327	−0.013	−0.058	−0.061
916.623	0.8959	−0.012	−0.020	−0.022
497.431	0.9418	−0.0076	−0.0080	−0.0090
264.105	0.9687	−0.0042	−0.0033	−0.0039
Std. dev. (18 pt.)		0.026	0.100	0.115
38.4% methane at 25°C.				
11,764.563	1.7279	−0.11	−0.19	−0.23
1,955.775	0.5580	−0.0030	−0.42	−0.39
1,189.713	0.6593	−0.016	−0.14	−0.13
737.574	0.7939	−0.012	−0.044	−0.041
423.983	0.8864	−0.0085	−0.015	−0.014
231.381	0.9396	−0.0051	−0.0061	−0.0056
Std. dev. (18 pt.)		0.031	0.227	0.222
38.4% methane at 50°C.				
11,821.134	1.6567	−0.050	−0.12	−0.16
2,421.685	0.6588	−0.0081	−0.31	−0.30
1,374.401	0.7258	−0.011	−0.10	−0.10
812.618	0.8331	−0.010	−0.032	−0.031
455.889	0.9072	−0.0069	−0.010	−0.010
245.982	0.9502	−0.0038	−0.0036	−0.0034
Std. dev. (18 pt.)		0.016	0.174	0.185
38.4% methane at 75°C.				
11,998.476	1.6301	−0.075	−0.16	−0.19
2,830.143	0.7454	+0.0033	−0.23	−0.23
1,534.264	0.7834	−0.011	−0.077	−0.076
875.862	0.8670	−0.010	−0.024	−0.026
482.517	0.9259	−0.0070	−0.0083	−0.0088
258.132	0.9602	−0.0040	−0.0031	−0.0034
Std. dev. (18 pt.)		0.021	0.178	0.179
18.4% methane at 25°C.				
11,817.669	1.7525	−0.011	−0.079	−0.16
1,509.396	0.4355	−0.022	−0.55	−0.51
1,026.253	0.5762	−0.0065	−0.18	−0.17
680.590	0.7434	−0.0051	−0.051	−0.046
403.531	0.8576	−0.0033	−0.015	−0.012
223.449	0.9240	−0.0020	−0.0043	−0.0033
2,894.576	0.5843	+0.078	−0.70	−0.66
1,233.868	0.4846	−0.0028	−0.35	−0.32
862.717	0.6593	−0.0067	−0.10	−0.093
540.493	0.8037	−0.0046	−0.029	−0.025
308.773	0.8934	−0.0028	−0.0083	−0.0067
167.615	0.9436	−0.0015	−0.0025	−0.0017
Std. dev. (24 pt.)		0.021	0.288	0.256
18.4% methane at 50°				
11,720.820	1.6682	+0.0019	−0.097	−0.17
2,005.647	0.5550	+0.024	−0.41	−0.38
1,221.971	0.6575	−0.0045	−0.13	−0.12
757.549	0.7925	−0.0056	−0.036	−0.033
435.012	0.8848	−0.0039	−0.0099	−0.0089
237.259	0.9383	−0.0022	−0.0025	−0.0022
2,866.280	0.6176	+0.055	−0.52	−0.50
1,444.130	0.6050	−0.0011	−0.21	−0.19
916.016	0.7461	−0.0062	−0.060	−0.055
540.335	0.8557	−0.0050	−0.017	−0.015
299.478	0.9221	−0.0031	−0.0047	−0.0041
160.164	0.9588	−0.0016	−0.0013	−0.0010
Std. dev. (24 pt.)		0.019	0.217	0.185
18.4% methane at 75°C.				
11,607.333	1.6180	−0.071	−0.22	−0.28
2,424.557	0.6559	+0.016	−0.30	−0.29
1,384.376	0.7270	−0.0057	−0.095	−0.091
818.485	0.8342	−0.0069	−0.027	−0.026
459.023	0.9080	−0.0050	−0.0076	−0.0075
247.663	0.9509	−0.0030	−0.0023	−0.0024
2,962.640	0.6832	+0.024	−0.37	−0.35
1,564.158	0.7000	−0.0038	−0.13	−0.12
933.498	0.8109	−0.0072	−0.036	−0.035
529.930	0.8934	−0.0049	−0.0096	−0.0094
288.083	0.9427	−0.0034	−0.0030	−0.0030
152.681	0.9697	−0.0018	−0.0008	−0.0009
Std. dev. (24 pt.)		0.021	0.178	0.179

$\Delta Z_{\mathrm{R\text{-}K}} = (Z_{\mathrm{R\text{-}K}} - Z_{\mathrm{Expt}})$; $\Delta Z_{\mathrm{B\text{-}W\text{-}R}} = (Z_{\mathrm{B\text{-}W\text{-}R}} - Z_{\mathrm{Expt}})$; $\Delta Z_{\mathrm{G\text{-}B\text{-}W\text{-}R}} = (Z_{\mathrm{G\text{-}B\text{-}W\text{-}R}} - Z_{\mathrm{Expt}})$.

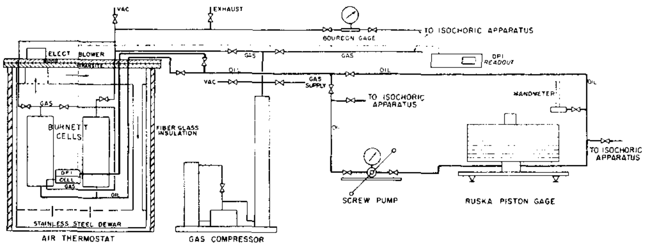

Fig. 1. Schematic diagram of Burnett apparatus.

Table 4. Estimated Error for Experimental Compressibility Factors at 95% Confidence Level

Temp., °C.	Estimated error as % of Z 99% methane	78.8% methane	57.2% methane	38.4% methane	18.4% methane	99.9% ethylene
25	0.15	0.04	0.12	0.07	0.36	0.68
50	0.03	0.03	0.05	0.03	0.05	0.27
75	0.05	0.06	0.03	0.04	0.77	0.04

A 100 ohm platinum resistance thermometer placed in the middle of the air thermostat between the two bombs was used as the sensing element for a current adjusting type of controller. The controller with three modes of control (proportional, rate, and reset) adjusted the voltage to the control heaters. With this arrangement, the air thermostat was maintained at the desired temperature to ±0.01°C.

A four lead, platinum resistance thermometer calibrated by the National Bureau of Standards was used to measure the temperature of the air thermostat. The resistance of the thermometer was determined with a bridge by using a ballastic galvanometer to the nearest 0.0001 ohm (0.001°C.).

Bombs

The two high pressure bombs of equal volume which were constructed of type 303 stainless steel, have been described previously by McMath (*19, 20*).[*] The bombs were connected to the vacuum system, gas charging system, and DPI cell by using ⅛-in. stainless steel tubing and ⅛-in. stainless steel needle valves. Also, a high pressure ⅛-in. stainless steel needle vavle was used as the expansion valve between the two bombs. A hand operated piston type of gas compressor was used in charging the bombs with gas. The pressure jacket was connected to the oil system of the screw pump (Figure 1) so that the pressure in the jacket of the bombs could be maintained at the proper valve to account for the pressure distortion of the bombs (*19*).

Pressure Measurement

A dual range piston gauge was used to determine pressure on the gas sample. A screw pump was used to pressure the oil, and a DPI cell was located between the oil and the gas sample (Figure 1). A differential pressure of ±0.0002 lb./sq. in. could be detected with the DPI cell and readout. When the effects of pressure and temperature on the area of the piston are taken into account, pressures can be measured to an accuracy of one part in 10,000.

Barometric pressures were measured with a servo-nulling gauge.

Gas Samples

Six bottles of gases were supplied for this research by Phillips Petroleum Company, who analyzed the blends by mass spectroscopy and reported the compositions to the nearest 0.1 mole %. These compositions, which are given in Table 1, were checked on a gas chromatograph to this same accuracy, that is, 0.1 mole %.

PROCEDURE

Before the gas compressor or the bombs were charged with a gas sample, the apparatus was evacuated, flushed with a gas sample, and reevacuated. While bomb V_1 was filled, the oil side pressure of the DPI cell was maintained at least 500 lb./sq. in. above the gas side pressure. Overpressuring the DPI cell on the oil side when filling or emptying the bombs was routine.

After the gas sample had attained thermal equilibrium with the air thermostat, a preliminary pressure measurement was made with the piston gauge. The jacket pressure was then set at 0.8024 of the gas sample pressure. (This value for the jacket pressure minimizes the pressure distortion of the inner volume of the bombs.) The piston and weights were rotated for about 15 to 20 min. before the final value of the gas sample pressure was determined.

Before the first expansion, the gas pressure was measured with the expansion valve closed and a vacuum of 50μ Hg in bomb V_2. The remaining pressure measurements were made before each expansion with the expansion valve open less than ⅛ of a revolution. The pressure change caused by closing the expansion valve was not detected by the DPI instrument.

Between expansions, the gas sample was allowed to reattain thermal equilibrium with the air thermostat. Long periods of time were required to attain thermal equilibrium after an expansion. These long periods were due to the low heat capacity of air and the slow rate of heat transfer from the air to the bombs.

EXPERIMENTAL RESULTS

In preparation for the derivation of compressibility factors and virial coefficients, the observed data were converted to temperatures and pressures. Temperatures were calculated from the piston gauge loadings and the barometric pressure. These calculations were based on the calibration data for each instrument and were made via a digital computer. The compressibility factors and virial coefficients were calculated from the expansion data in

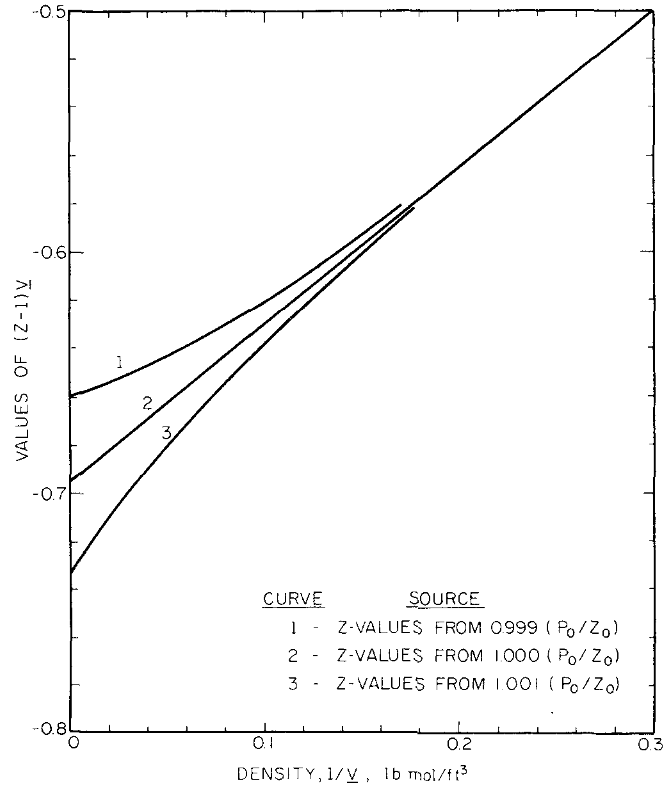

Fig. 2. Effect of (P_0/Z_0) on $(Z-1)V$ for methane at 25°C.

---

[*] See Acknowledgment.

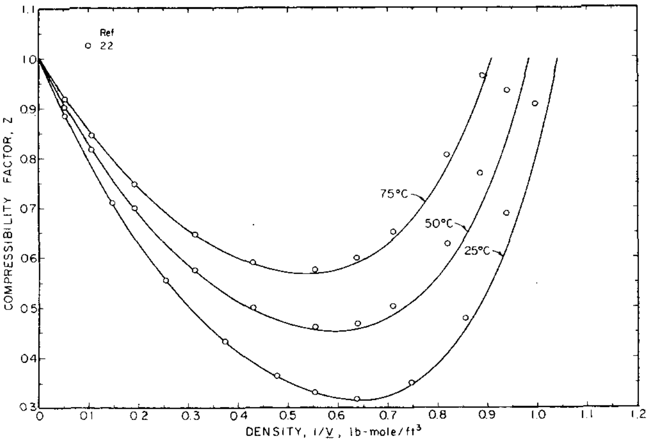

Fig. 3. Comparison of this work with literature for methane.

three major steps: determination of cell constant, determination of Z_0 and compressibilities Z_j's, and virial coefficients.

Cell Constant

The first step was to determine the cell constant N from the expansion data for each gas system at each isotherm. As shown by Equation (3), the cell constant can be determined by extrapolating the pressure ratios P_{j-1}/P_j (P_{j-1} = pressure before j^{th} expansion, and P_j = pressure after expansion) to zero pressure. Plots of the pressure ratios were prepared to establish the range of the pressure data to be used in curve fitting these pressure ratios to a power series in pressure for determining the cell constant. Data below 150 lb./sq.in.abs. scattered badly. This scatter was probably due to difficulty in measuring lower pressures with the dead weight piston gauge. The pressure range chosen for the curve fit ranged from 150 to 1,500 lb./sq.in.abs. for methane and from 150 to 1,000 lb./sq.in.abs. for ethylene, with ranges for the methane-ethylene mixtures falling in between. These plots of the pressure ratios vs. pressure were also used to check the curve-fitting results.

TABLE 5. SECOND VIRIAL COEFFICIENTS VIA ALTERNATE METHODS

Units: cc./g.-mole

Gas system	Slope intercept	Curve fit
	Values of B at 25°C.	
Methane	−42.88 ± 1.5	−42.70 ± 2.3
80-20	−55.39 ± 1.3	−55.93 ± 0.62
60-40	−72.35 ± 3.0	−75.20 ± 2.6
40-60	−90.66 ± 1.5	−92.40 ± 1.0
20-80	−116.90 ± 1.4	−128.30 ± 3.9
Ethylene	−145.60 ± 4.8	−152.50 ± 6.0
	Values of B at 50°C.	
Methane	−33.22 ± 1.0	−33.46 ± 0.30
80-20	−43.74 ± 0.5	−43.87 ± 0.71
60-40	−60.54 ± 0.4	−59.50 ± 2.1
40-60	−77.47 ± 0.1	−77.60 ± 1.0
20-80	−93.32 ± 0.7	−98.32 ± 0.39
Ethylene	−120.40 ± 1.3	−122.10 ± 2.4
	Values of B at 75°C.	
Methane	−26.54 ± 1.1	−25.69 ± 0.90
80-20	−34.07 ± 1.1	−34.64 ± 1.4
60-40	−49.85 ± 0.4	−50.12 ± 0.93
40-60	−64.30 ± 0.2	−65.60 ± 0.62
20-80	−82.03 ± 0.8	−81.60 ± 5.2
Ethylene	−100.80 ± 1.1	−101.50 ± 0.80

TABLE 6. THIRD VIRIAL COEFFICIENTS VIA ALTERNATE METHODS

Units: (cc./g.-mole)^2 × 10^{-3}

Gas system	Slope intercept	Curve fit
	Values of C at 25°C.	
Methane	2.39 ± 0.8	2.45 ± 0.87
80-20	2.68 ± 0.6	2.88 ± 0.21
60-40	3.25 ± 1.6	4.70 ± 1.2
40-60	4.10 ± 0.9	4.69 ± 0.37
20-80	6.54 ± 0.6	12.60 ± 3.2
Ethylene	9.79 ± 2.6	14.30 ± 4.9
	Values of C at 50°C.	
Methane	1.78 ± 0.4	1.90 ± 0.12
80-20	2.15 ± 0.2	2.11 ± 0.24
60-40	3.21 ± 0.09	2.43 ± 0.81
40-60	4.31 ± 0.08	4.32 ± 0.40
20-80	5.71 ± 0.07	5.51 ± 0.19
Ethylene	7.05 ± 0.4	7.50 ± 1.5
	Values of C at 75°C.	
Methane	1.96 ± 0.5	1.40 ± 0.42
80-20	1.71 ± 0.4	1.83 ± 0.48
60-40	2.82 ± 0.09	2.96 ± 0.48
40-60	3.67 ± 0.07	4.29 ± 0.35
20-80	4.70 ± 0.4	4.82 ± 0.70
Ethylene	5.98 ± 0.8	6.32 ± 0.47

The pressure ratio data selected were fitted to a power series in pressure by using the number of terms which gave the best fit as determined by the minimum value of the standard estimate of error. Equation (5) is the expression used in this step:

$$\frac{P_{j-1}}{P_j} = a_0 + a_1P_j + a_2P_j^2 + \dots \qquad (5)$$

The cell constant N, defined above, is the zero pressure intercept of Equation (5). Values of N were determined in this way for each isotherm and mixture studied. These N values are given in Table 2. These values represent the cell constant that best describes the pressure ratio data at low pressures for each isotherm of each gas system. The variation of the cell constant with temperature was expected, but the variation with composition was unexpected. This dependence on composition is probably due to the technique used in evaluating the cell constant from the pressure ratio data. The plots of the pressure ratios P_{j-1}/P_j vs. pressure P_j showed that the isotherms for methane had much less curvature than those for ethylene. This difference in curvature is apparently reflected in the changing values of the cell constant shown in Table 2. Barieau and Dalton (*1*) have described a method of determining the cell constant and the initial compressibility factor Z_0, that is, before the first expansion. Their method uses the expansions over the entire pressure range instead of only the low pressure data. However, the Barieau-Dalton method became available too late for use in this work.

EXPERIMENTAL COMPRESSIBILITY FACTORS

The second major step in data processing was to determine the initial compressibility factor Z_0 of the starting fluid for each run. As shown by Equation (4), P_0/Z_0 (P_0

= pressure before first expansion) can be evaluated by extrapolating $N^j P_j$ to zero pressure. Plots of $N^j P_j$ vs. P_j were prepared for each run to serve as a check for determining P_0/Z_0 by curve fitting. The low pressure data (same range of pressure data as used for determining cell constant) were fitted to a power series in pressure, given below as Equation (6), by using the number of terms which gave the best fit to the data:

$$N^j P_j = b_0 + b_1 P_2 + b_2 P_j^2 + \ldots \qquad (6)$$

By using the value of the cell constant and P_0/Z_0 for each run, the compressibility factors Z_j's were calculated from the pressure values P_j's by using Equation (2). By using these Z values, plots of $(Z - 1)\underline{V}$ vs. $1/\underline{V}$ were prepared.

A strong dependence of the slope on the exact P_0/Z_0 value was found. This dependence is illustrated in Figure 2 for a ±0.1% change in the value of P_0/Z_0. A value of P_0/Z_0 either too high or too low caused the plot of $(Z - 1)\underline{V}$ vs. $1/\underline{V}$ to be nonlinear at low densities. The value of P_0/Z_0 which led to a linear plot of $(Z - 1)\underline{V}$ vs. $1/\underline{V}$ at low densities was considered the correct value.

Each value of P_0/Z_0 was determined initially by curve fitting the $N^j P_j$ values and was adjusted to get the smoothest and most consistent representation possible of the experimental data using the following procedure to make the adjustments: the low pressure compressibility data (that is, 150 to 1,500 or 1,000 lb./sq.in.abs.) obtained from the initially found P_0/Z_0 value, were fitted to the following form of the virial equation and the sum-of-squares of the deviations were obtained:

$$(Z - 1)\underline{V} = B(T) + C(T)/\underline{V} + D(T)/\underline{V}^2 + \ldots \qquad (7)$$

The value of P_0/Z_0 was changed by an increment, for which new compressibility factors were calculated and fitted to Equation (7), obtaining the sum of squares of the deviations. The value of P_0/Z_0 was adjusted again and again until the sum of squares from the fit to Equation (7) was a minimum, and this value of P_0/Z_0 was used to calculate the compressibility factors that are reported as the experimental results of this work.

TABLE 7. SECOND VIRIAL COEFFICIENTS CORRECTED FOR IMPURITIES

Composition, mole %	Temp., °C.	B, cc./g.-mole
Methane	25	−41.57
	50	−32.04
	75	−25.49
Ethylene[*]	25	−145.6
	50	−120.4
	75	−100.8
79.2% methane 20.8% ethylene	25	−52.51
	50	−41.19
	75	−31.81
57.4% methane 42.6% ethylene	25	−70.29
	50	−58.74
	75	−48.28
38.5% methane 61.5% ethylene	25	−89.85
	50	−76.51
	75	−63.46
18.4% methane[*] 81.6% ethylene	25	−116.9
	50	−98.32
	75	−82.02

[*] Note: No corrections made for these gases.

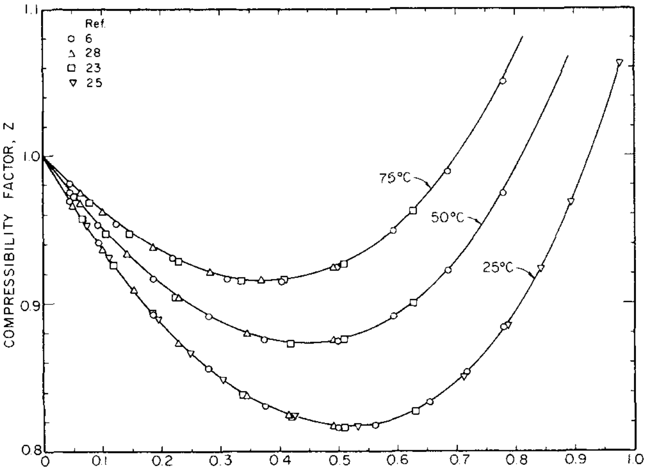

Fig. 4. Comparison of this work with literature for ethylene.

Derived Z Values

The resulting compressibility factors for methane, ethylene, and four binary mixtures (see Table 1 for compositions) at 25°, 50°, and 75°C. were determined from the isothermal expansion data (*14*) as described above. Three series of expansions were made for each of the six gases, with an additional series made for ethylene and the 20 to 80 methane-ethylene mixture to cover the pressure range 150 to 12,000 lb./sq.in.abs. Part of the experimental compressibility factors are shown in Table 3.[*]

These experimental compressibility factors were compared with the Redlich-Kwong (R-K), Benedict-Webb-Rubin (B-W-R), and the Edmister et al. (*8*) generalized B-W-R equations of state. The two constants for the R-K equation were determined by using the critical properties of methane and ethylene. The eight constants for the B-W-R equation were taken from Benedict et al. (*2*) and Eakin and Ellington (*7*). The generalized constants for the B-W-R equations were calculated by using critical properties and the acentric factor (*8, 11*). The deviations between the empirical equations of state and the experimental data are summarized in Table 3.

The standard deviations for the R-K equation varied from 0.016 to 0.064 over the range of the experimental data, while the standard deviations for the two B-W-R equations varied from 0.051 to 0.33. The variations seemed to be random, with no particular dependence on composition. If the Redlich-Kwong equation is restricted to densities below 0.65 lb.-mole/cu.ft. (pressures below 3,100 lb./sq.in.abs.) for methane and below 0.5 lb.-mole/cu.ft. (pressures below 1,000 lb./sq.in.abs.) for ethylene, the

---

[*] The complete Table 3 has been deposited as document 01202 with the ASIS National Auxiliary Publications Service, c/o CCM Information Sciences, Inc., 22 W. 34th St., New York 10001 and may be obtained for $2.00 for microfiche or $5.00 for photocopies.

Table 8. Second Virial Cross Coefficients

Temp., °C.	B_{12}, cc./g.-mole
−4.44*	−89.8*
4.44*	−78.6*
15.56*	−71.5*
25.00	−61.15
50.00	−53.99
75.00	−43.75

* McNath (*19*).

R-K compressibility factors are within ±0.02 of the experimental data. In contrast, the B-W-R and the generalized B-W-R would have to be restricted to densities below 0.25 lb.-mole/cu.ft. (pressures below 1,200 lb./sq.in.abs.) for methane and below 0.12 lb.-mole/cu.ft. (pressures below 550 lb./sq.in.abs.) for ethylene to be within ±0.02 of the experimental data. Similar results were found when the equations were compared with the mixture data. The combination rules used with these empirical equations of state led to as satisfactory results for the mixtures as obtained for the pure components.

VIRIAL COEFFICIENTS VIA CURVE FITTING

The experimental compressibility data were curve fitted to the Leiden form of the virial equation of state, shown below, truncating the series after the term which gave the best fit (minimum value for standard estimate of error):

$$Z = 1 + B(T)/\underline{V} + C(T)/\underline{V}^2 + D(T)/\underline{V}^3 + \ldots \quad (8)$$

The estimated error expressed relative to the mean value of Z used in the fit are shown in Table 4.

The methane and ethylene compressibility data were compared with data available in the literature in Figures 3 and 4. Only a portion of each investigators' data is shown. An attempt was made to show by the width of the curve the 95% confidence interval for the curve fits of the virial equation of state to the experimental data, but this was not practical as the curves were of widths varying from 0.001 to 0.05 units of Z.

At the 95% confidence level, the methane compressibility factor data from the literature agree at 25° and 50°C. with experimental data. Only the low pressure data (to 1,500 lb./sq.in.abs.) at 75°C. fall within the 95% confidence interval. The 25°C. data of Michels and Geldermans (22) for ethylene fall in this interval up to a density of 0.6 lb.-mole/cu.ft. (pressure to 1,100 lb./sq.in.abs.). Only the lower density data (to 0.2 lb.-mole/cu.ft.) fall within the band for 50° and 75°C.

The differences between the experimental data of this work and the literature values increase with increasing pressure, particularly for ethylene. This increasing divergences with pressure was partially due to differences in the piston gauges used for measuring pressure and the curvature of the isothermal expansion ratio (P_{j-1}/P_j) data. The curvature of the isothermal expansion data for ethylene at low pressure made it difficult to evaluate the cell constant N and P_0/Z_0. Also, pressure measurements below 150 lb./sq.in.abs. were in general unreliable with the piston gauge.

VIRIAL COEFFICIENTS VIA SLOPE INTERCEPT

Second and third virial coefficients were derived from the compressibility factor data by using the slope intercept method programmed for a digital computer. An initial value for the second virial coefficient was obtained from the P_0/Z_0 adjustment procedure described previously. This data was curve fitted by using the following rearrangement of the virial equation:

$$[(Z-1)\underline{V} - B(T)]\underline{V} = C(T) + D(T)/\underline{V} + E(T)/\underline{V}^2 + \ldots \quad (9)$$

The value of $B(T)$ was adjusted until the curve fit to Equation (9) gave a minimum sum of squares. This procedure is analogous to the graphical slope intercept method where the value of $B(T)$ is adjusted until the plot of $[(Z-1)\underline{V} - B(T)]\underline{V}$ vs. $1/\underline{V}$ becomes linear at low densities.

The third virial coefficient obtained from the adjustment procedure for $B(T)$ was adjusted similarly by using the following equation for the curve fit:

$$\{[(Z-1)\underline{V} - B(T)]\underline{V} - C(T)\}\underline{V} = D(T) + E(T)/\underline{V} + F(T)/\underline{V}^2 + \ldots \quad (10)$$

The results of the computer calculations were checked graphically.

The second and third virial coefficients derived from the experimental compressibility data by using the slope intercept method and curve fitting to the Leiden form of the virial equation of state are presented in Tables 5 and 6. The nominal compositions refer to the gas compositions shown in Table 1. The estimated error for the second virial coefficients varied from ±0.2 to ±4.8 cc./g.-mole for the slope intercept method and from ±0.3 to ±6.0 cc./g.-mole for the curve fit. The estimated error for the third virial coefficients varied from $\pm 0.07 \times 10^3$ to $\pm 2.6 \times 10^3$ (cc./g.-mole)^2 for the slope intercept method and from $\pm 0.12 \times 10^3$ to $\pm 4.9 \times 10^3$ (cc./g.-mole)^2 for the curve fit. Comparison of the two methods (Tables 5 and 6) shows that both give essentially the same values within the estimated error for the second and third virial coefficients.

The second and third virial coefficients were evaluated from the constants for the R-K, B-W-R, and the generalized B-W-R equation of state. The expressions for the B-W-R and generalized B-W-R are

$$B(T) = B_0 - A_0/(RT) - C_0/(RT)^3 \quad (11)$$

$$C(T) = b - a/(RT) + C/(RT)^3 \quad (12)$$

The expressions for the R-K equation are

$$B(T) = b - a/(RT^{1.5}) \quad (13)$$

$$C(T) = b^2 + ab/(RT^{1.5}) \quad (14)$$

In general, the second and third virial coefficients calculated from the constants for the R-K, B-W-R, and generalized B-W-R equations do not predict the experimental values within the estimated error of the experimental data. Considering that the R-K equations has only two constants, this equation did remarkably well in predicting the second virial coefficients in comparison with the B-W-R equation. In this case, part of the deviations from the experimental virial coefficients is a reflection of the deviations between the equations and the experimental compressibility data.

CROSS COEFFICIENTS

The gases used in this study contained impurities (Table 1). The second virial coefficients were corrected for these impurities by using the following relationship for n-component mixture (10):

$$B_M(T) = \sum_i^n \sum_j^n B_{ij}(T)\, x_i x_j \qquad (15)$$

The values for the pure components and the interaction coefficients (B_{ij}) from the literature (*11*) were used when available. The other coefficients were estimated by using a correlation by Huff and Reed (*11*). The corrected second virial coefficients and the corresponding compositions are shown in Table 7. The corrections varied from 0.84 to 2.88 cc./g.-mole and were approximately the same as the estimated error for the second virial coefficients.

For a binary system, Equation (15) reduces to

$$B_M(T) = x_1 B_{11}(T) + 2x_1x_2B_{12}(T) + x_2^2B_{22}(T) \qquad (16)$$

The second virial coefficient data and compositions shown in Table 7 were used with Equation (16) to evaluate B_{12} by curve fitting. The results are shown in Table 8 along with values by McMath (*19*).

CONCLUSIONS

Comparison of the experimental compressibility data with three empirical equations of state showed that the two constant R-K equations did better at predicting the experimental data than the more complicated B-W-R or generalized B-W-R. However, none of the three were satisfactory in predicting the experimental data over the entire pressure range.

In general, the experimental compressibility data for methane agreed with literature values for the 25° and 75°C. isotherms. Only low pressure data for methane at 75°C. (below 1,500 lb./sq.in.abs.) and for ethylene at 25°, 50°, and 75°C. (below 1,100 lb./sq.in.abs.) agreed with literature values.

Two methods of deriving virial coefficients from compressibility data were compared. The slope intercept method and the curve fit method give essentially the same values for the second and third virial coefficients. Second and third virial coefficients calculated from the constants for the R-K, B-W-R, and generalized B-W-R did not agree with the experimental values.

ACKNOWLEDGMENT

This investigation was supported by grants from the Petroleum Research Fund of ACS and the National Science Foundation. The gas samples were furnished by Phillips Petroleum Company. The high pressure bombs used in this work, as well as the one used by McMath (*19, 20*), were made from a design by J. E. Miller of the Helium Research Center, Amarillo, Texas (Bureau of Mines Information Circular 8350).

NOTATION

a, A_0 = constants in equations of state
b, B_0 = constants in equations of state
a_0, a_1, a_2, etc. = constants in empirical equation for P_{j-1}/P_j
b_0, b_1, b_2, etc. = constants in empirical equation for N^jP_j
$B(T)$, $C(T)$, $D(T)$ = second, third, fourth, etc., virial coefficients
$B_{ij}(T)$ = interaction second virial coefficient
c, C_0 = constants in equation of state
$N = \dfrac{V_1 + V_2}{V_1}$ = volume ratioi of expansion cells
$\underline{V}$ = molar volume
x = mole fraction
Z = compressibility factor, $P\underline{V}/RT$
γ = constants in equation of state

Subscripts

i = component of a mixture
j = component of a mixture
j = number of expansions
M = mixture

LITERATURE CITED

1. Barieau, R. C., and B. J. Dalton, *U.S. Bureau of Mines RI 7020* (Sept., 1967).
2. Benedict, Manson, G. B. Webb, and L. C. Rubin, *Chem. Eng. Progr.*, **47**, No. 8, 419 (1951).
3. Burnett, E. S., *J. Appl. Mech.*, **3**, A-136 (1936).
4. Canfield, F. B., T. W. Leland, and Riki Kobayashi, "Advances in Cryogenic Engineering," Vol. 8, p. 146, Plenum Press, New York (1963).
5. Cawood, W., and H. S. Patterson, *J. Chem. Soc. (London)*, **1**, 619 (1933).
6. Douslin, D. R., R. H. Harrison, R. T. Moore, and J. P. McCullough, *J. Chem. Eng. Data*, **9**, 358 (1964).
7. Eakin, B. E., and R. T. Ellington, "Papers of the Symposium on Thermal Properties," p. 195 Purdue Univ., Lafayette, Ind. (1959).
8. Edmister, W. C., J. Vairogs, and A. J. Klekers, *AIChE J.*, **14**, 479 (1968).
9. Fruth, F. A., and T. T. H. Verschoyle, *Proc. Royal Soc.*, **130A**, 453 (1931).
10. Hirschfelder, J. C., C. F. Curtis, and R. B. Bird, "Molecular Theory of Gases and Liquids," Wiley, New York (1954).
11. Huff, J. A., and T. M. Reed, III, *J. Chem. Eng. Data*, **8**, 306 (1963).
12. Keyes, F. G., and H. G. Burks, *J. Am. Chem. Soc.*, **49**, 1403 (1927).
13. Kvalnes, H. M., and V. L. Gaddy, *ibid.*, **53**, 394 (1931).
14. Lee, R. C., Ph.D. thesis, Okla. State Univ., Stillwater (1969).
15. MacCormack, K. E., and W. G. Schneider, *J. Chem. Phys.*, **18**, 1269 (1950).
16. *Ibid.*, **19**, 845 (1951).
17. Matthews, C. J., and C. O. Hurd, *Trans. Am. Inst. Chem. Engrs.*, **42**, 55 (1946).
18. Masson, I., and L. G. F. Dolley, *Proc. Royal Soc.*, **103A**, 524 (1923).
19. McMath, H. G., Jr., Ph.D. thesis, Okla. State Univ., Stillwater (1967).
20. ———, and W. C. Edmister, *AIChE J.*, **15**, 370 (May, 1969).
21. Michels, A., J. DeGruyter, and F. Niesen, *Physica*, **3**, 346 (1936).
22. Michels, A., and M. Geldermans, *ibid.*, **9**, 967 (1942).
23. Michels, A., and G. W. Nederbragt, *ibid.*, **3**, 569 (1936).
24. Mueller, W. H., T. W. Leland, Jr., and Riki Kobayashi, *AIChE J.*, **7**, 267 (1961).
25. Olds, R. H., H. H. Reamer, B. H. Sage, and W. H. Lacey, *Ind. Eng. Chem.*, **35**, 922 (1943).
26. Pavlovich, N. V., and D. L. Timrot, *Teploinergetika*, **5**, 69 (1958).
27. Pfennig, H. W., and J. J. McKelta, *Petrol. Refiner*, **36**, No. 11, 309 (1957).
28. Schamp, H. W., Jr., E. A. Mason, A. C. B. Richardson, and A. Altman, *Phys. Fluids*, **1**, 329 (1958).
29. Schneider, W. G., *Can. J. Res.*, **27B**, 339 (1940).
30. ———, and J. A. H. Duffie, *J. Chem. Phys.*, **17**, 751 (1949).
31. Silberberg, D. H., K. A. Kobe, and J. J. McKelta, *J. Chem. Eng. Data*, **4**, 314 (1959).
32. Vennix, A. J., Ph.D. thesis, Rice Univ., Houston, Tex. (1966).
33. Walters, R. J., J. H. Tracht, E. B. Weinberger, and J. K. Rodgers, *Chem. Eng. Progr.*, **50**, 511 (1954).
34. Witonsky, R. J., and J. G. Miller, *J. Am. Chem. Soc.*, **85**, 282 (1963).
35. York, R., and E. F. White, *Trans. Am. Soc. Mech. Engrs.*, **40**, 227 (1944).

Manuscript received January 31, 1969; revision received May 5, 1969; paper accepted May 7, 1969. Paper presented at AIChE New Orleans meeting.